LCC-0105
CBP Tec Note-266
October 2002

Linear Collider Collaboration Tech Notes

Effects of Systematic Multipole Errors on the Dynamic Aperture of the NLC Main Damping Rings

A. Wolski, J.-Y. Jung

Lawrence Berkeley National Laboratory
University of California
Berkeley, CA

Abstract: Recent work on designs of dipoles, quadrupoles and sextupoles for the NLC Main Damping Ring has led to estimates of the systematic multipole components in the fields of these magnets. We report on studies of the effects of these multipoles on the dynamic aperture of the damping ring, and show that the systematic multipole components in the present magnet designs are unlikely to be a severe limitation.

LCC-0105
CBP Tech Note-266

Effects of Systematic Multipole Errors on the Dynamic Aperture of the NLC Main Damping Ring

A. Wolski, J.-Y. Jung
Lawrence Berkeley National Laboratory

October 10th, 2002

Abstract

Recent work on designs of dipoles, quadrupoles and sextupoles for the NLC Main Damping Ring has led to estimates of the systematic multipole components in the 2-D fields of these magnets. We report on studies of the effects of these multipoles on the dynamic aperture of the damping ring, and show that the systematic multipole components in the present magnet designs are unlikely to be a severe limitation.

1 Introduction

A good dynamic aperture is needed in the NLC damping rings to ensure good injection efficiency. The design target for the main damping rings is a dynamic aperture of fifteen times the injected beam size for on-momentum particles [1]. The principal limitations on the dynamic aperture are the sextupole fields needed to correct the chromaticity, and possible non-linear components in the wiggler field. However, systematic and random higher order components in the dipoles, quadrupoles and sextupoles (the principal magnets) are also expected to limit the dynamic aperture.

Design work on permanent magnet and electromagnet options for the damping ring magnets has previously been reported [2]. Outline electromagnetic designs for the principal magnets have recently been completed. All magnets are based on normal conducting electromagnet technology, and the designs specify the poles, yokes and coils. The principal design constraints are the aperture, primary field strength and higher-order multipole components. Note that only two-dimensional designs have so far been studied; since the sextupoles in particular have short physical length compared to the pole-tip radius, it is possible that end effects could be significant, and careful studies and optimization of three-dimensional models will need to be performed.

Systematic higher-order multipole components of the magnetic field arise principally through limitations on the shape of the pole-tip; the components are constrained by the overall symmetry of the magnet, and are the same in every magnet of a given type. Random multipole components arise from variations in the construction of each individual magnet, and are not constrained by the symmetry of the design. Whereas systematic errors are known from the design, the random errors are not. Both types of error may be expected to limit the dynamic aperture of the lattice, and it is the purpose of the present note to quantify the effects of the systematic errors, and take an initial look at the random errors.

2 Systematic Multipole Components

2.1 Dipoles

The NLC MDR arc dipoles have a main field of 1.2 T, and a gradient of –6.605 T/m. In addition to the main arc dipoles, there are dipoles in the cells matching the arcs to the straight sections which have the same main field, but gradients of –6.175 T/m (injection/extraction straight) and –8.604 T/m (wiggler straight). There are also dipoles in the circumference-correction chicane, which have a field up to 1 T, and no gradient.

Designs have been produced so far only for the main arc dipoles. The aperture is specified to accept an inscribed circle of radius 20 mm centered on the beam; this allows for a beam pipe of 16 mm internal radius, 3 mm wall thickness and 1 mm clearance from the magnet. A cross section of the magnet with magnetic field lines is shown in Figure 1.

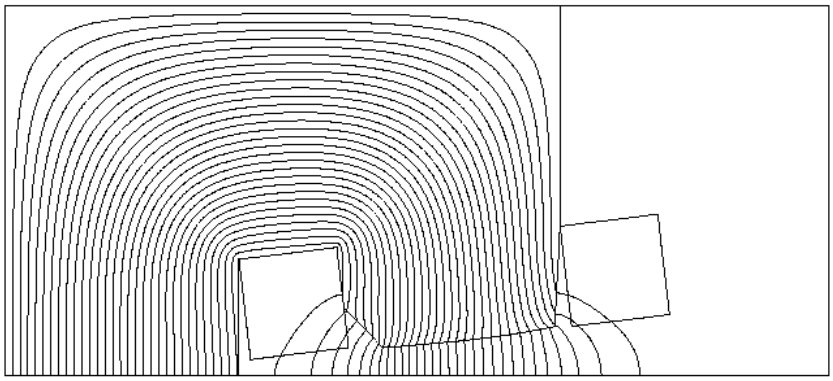

Figure 1

Dipole cross-section showing coil and field lines.

Multipole components are shown in Table 1. Note that the *k*-values for the components of a field are defined by:

$$k_n = \frac{1}{B\rho}\left.\frac{\partial^n B_y}{\partial x^n}\right|_{x=0}$$

where $B\rho$ is the beam rigidity, approximately 6.605 Tm at the 1.98 GeV nominal damping ring energy.

Table 1
Higher-order systematic multipoles in the NLC MDR main arc dipoles

n	k_n	$\Delta B/B_{\text{nominal}}$ at x = 0.01 m
0	0.1817 m^{-1}	-
1	-1.000 m^{-2}	-
2	-1.223 m^{-3}	-3.563×10^{-4}
3	-81.96 m^{-4}	-7.957×10^{-5}
4	-2.138×10^{4} m^{-5}	-5.627×10^{-5}
5	-1.879×10^{4} m^{-6}	-9.120×10^{-8}

The variation of the field from nominal is shown as a function of x in Figure 2. The variation of the field from the nominal at 20 mm horizontally from the beam axis is around 0.3%, and is dominated (as might be expected) by the sextupole component.

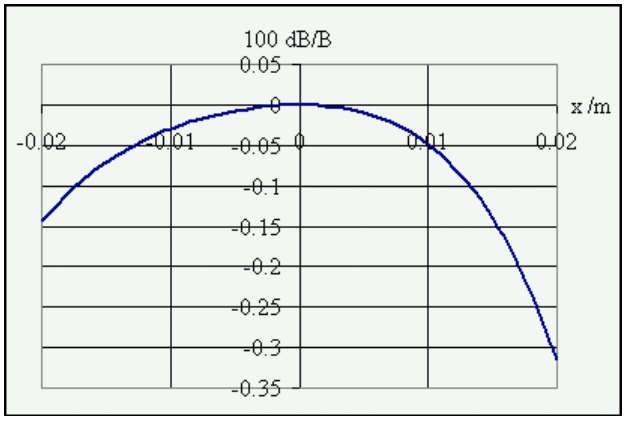

Figure 2

Field variation from nominal in a main arc dipole as a function of horizontal displacement from the orbit.

2.2 Quadrupoles

There are 18 families of quadrupoles in the present lattice design. However, the pole tip radius of all but two of the quadrupoles is 20 mm; the odd quadrupoles (in the injection/extraction regions) have a radius 30 mm. Generally, the field quality near the beam improves for larger pole-tip radius, so we treat the 30 mm quadrupoles as having the same field quality as the 20 mm quadrupoles. A cross-section of the quadrupole is shown in Figure 3.

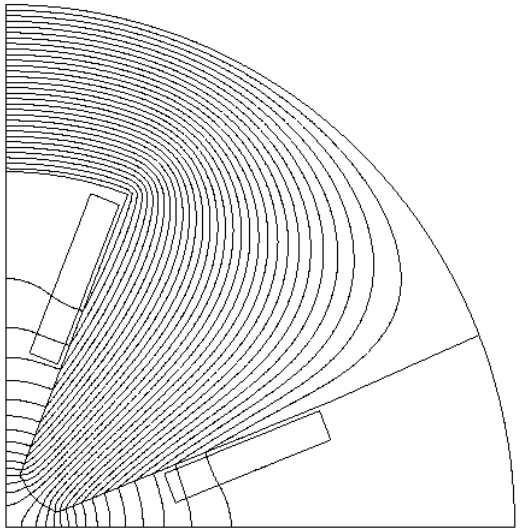

Figure 3

Quadrupole cross-section showing coil and field lines.

The higher-order multipole components and deviations from the quadrupole gradient are shown in Table 2. These values actually refer to a larger gradient than is actually neede in the present lattice design; values for the required quadrupoles are found by scaling the values in the table.

Table 2
Higher-order systematic multipoles in one family of NLC MDR quadrupoles.

n	k_n	$\Delta g/g_{\text{nominal}}$ at x = 0.016 m
1	$6.954\ \text{m}^{-2}$	-
5	$2.440\times10^{7}\ \text{m}^{-6}$	9.581×10^{-3}
9	$-8.358\times10^{16}\ \text{m}^{-10}$	-1.280×10^{-3}
13	$-4.513\times10^{28}\ \text{m}^{-14}$	-3.814×10^{-3}
17	$-5.138\times10^{39}\ \text{m}^{-18}$	-6.514×10^{-4}
21	$7.485\times10^{51}\ \text{m}^{-22}$	5.348×10^{-4}

The deviation from nominal quadrupole gradient as a function of horizontal offset from the beam axis is shown in Figure 4. Up to 16 mm (the internal radius of the beam pipe), the variation in the quadrupole gradient is less than 0.5%.

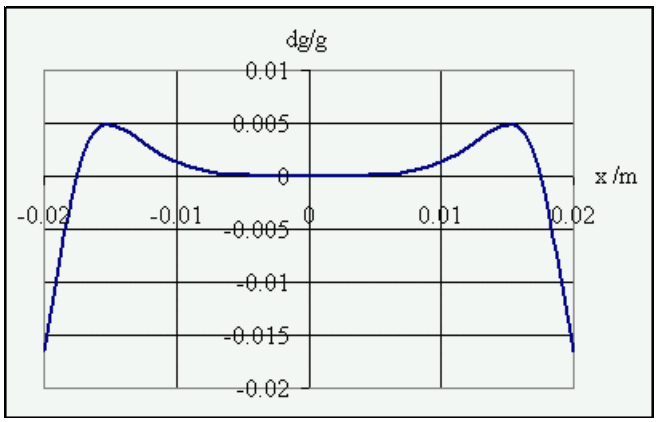

Figure 4

Quadrupole gradient variation as a function of horizontal displacement from the orbit.

2.3 Sextupoles

The present lattice design includes just two families of sextupoles; both have magnetic length 60 mm, and the aperture requirements specify a pole tip radius greater than 20 mm. To achieve the required field quality, the sextupole has been designed with a pole tip radius of 0.028 m. A cross-section is shown in Figure 5. We emphasize the fact that the present design is only two dimensional, and that this magnet has a pole-tip radius nearly half the magnetic length. Optimization of a full three-dimensional model of this magnet is therefore important, as is careful modeling of the dynamics in the magnet; it is planned to carry out this work in the future.

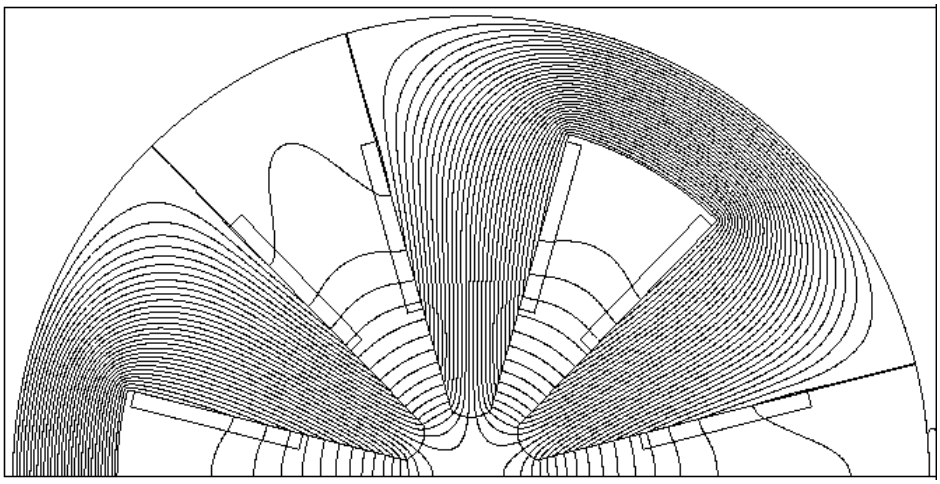

Figure 5

Sextupole cross-section showing coil and field lines.

Only one higher-order multipole component makes a significant contribution to the field. This component is given in Table 3, and the variation in the sextupole gradient is shown in Figure 6. Up to 16 mm, the variation in gradient is less than 1.7%. As in the case of the quadrupoles, values for the multipole components in the sextupoles used in the lattice are found by scaling the values in Table 3 by the sextupole strength.

Table 3
Higher-order systematic multipoles in one family of NLC MDR sextupoles.

n	k_n	$\Delta g_s / g_{s,\text{nominal}}$ at $x = 0.016$ m
2	454.2 m^{-3}	-
8	-3.291×10^{14} m^{-9}	-0.0169

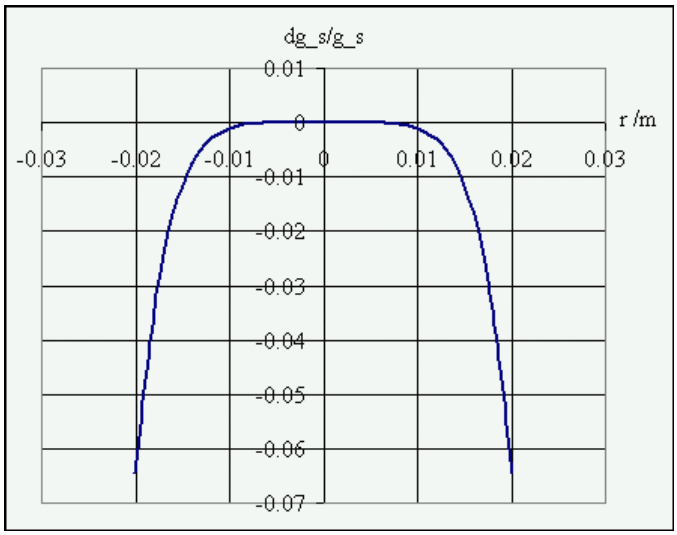

Figure 6

Sextupole gradient variation as a function of horizontal displacement from the orbit.

3 Random Multipole Components

Variation in construction from magnet to magnet leads to multipole components that are unique for each magnet. The random errors allow multipole components that in the case of systematic errors are forbidden by the symmetry of the design. At the present time, it is not known precisely how large the random errors are likely to be, nor is it known how they will be distributed between higher-order multipole components. To give some indication of the sensitivity of the lattice to random errors, we have taken those used for studies of the SPEAR 3 lattice [3], as shown in Table 4.

Table 4
Assumed higher-order random multipoles (rms values) in MDR main magnets.

Magnet	Multipole Component n	Reference Radius r_0 /m	Field Variation at r_0 $\Delta B_n/B_0$
Dipole	2 (sextupole)	0.03	10^{-4}
Quadrupole	3 (octupole)	0.032	5×10^{-4}
	4		10^{-4}
	5		10^{-4}
	6		5×10^{-4}
	7		10^{-4}
	8		10^{-4}
	9		10^{-4}
	10		5×10^{-4}
	11		10^{-4}
	12		10^{-4}
	13		10^{-4}
	14		5×10^{-4}
Sextupole	5	0.032	2×10^{-3}
	7		5×10^{-4}

Since the design and construction of the magnets for SPEAR 3 will certainly be different from those used in the damping rings, the values in Table 4 are not likely to be very realistic; however, we can assume that they give some indication of what one might expect.

4 Dynamic Effects

The dynamic aperture was calculated by tracking 500 turns of the full lattice in the beamline simulation code MERLIN. Only systematic and random higher-order multipole field errors were applied; nominal quadrupole and sextupole gradients were used, and no misalignments were applied. The results for on-momentum particles, and particles with ±0.5% momentum deviation, in the cases of no errors, systematic higher-order multipoles, and systematic and random higher-order multipoles, are shown in Figure 7. Note that we show a single representative seed for the random errors.

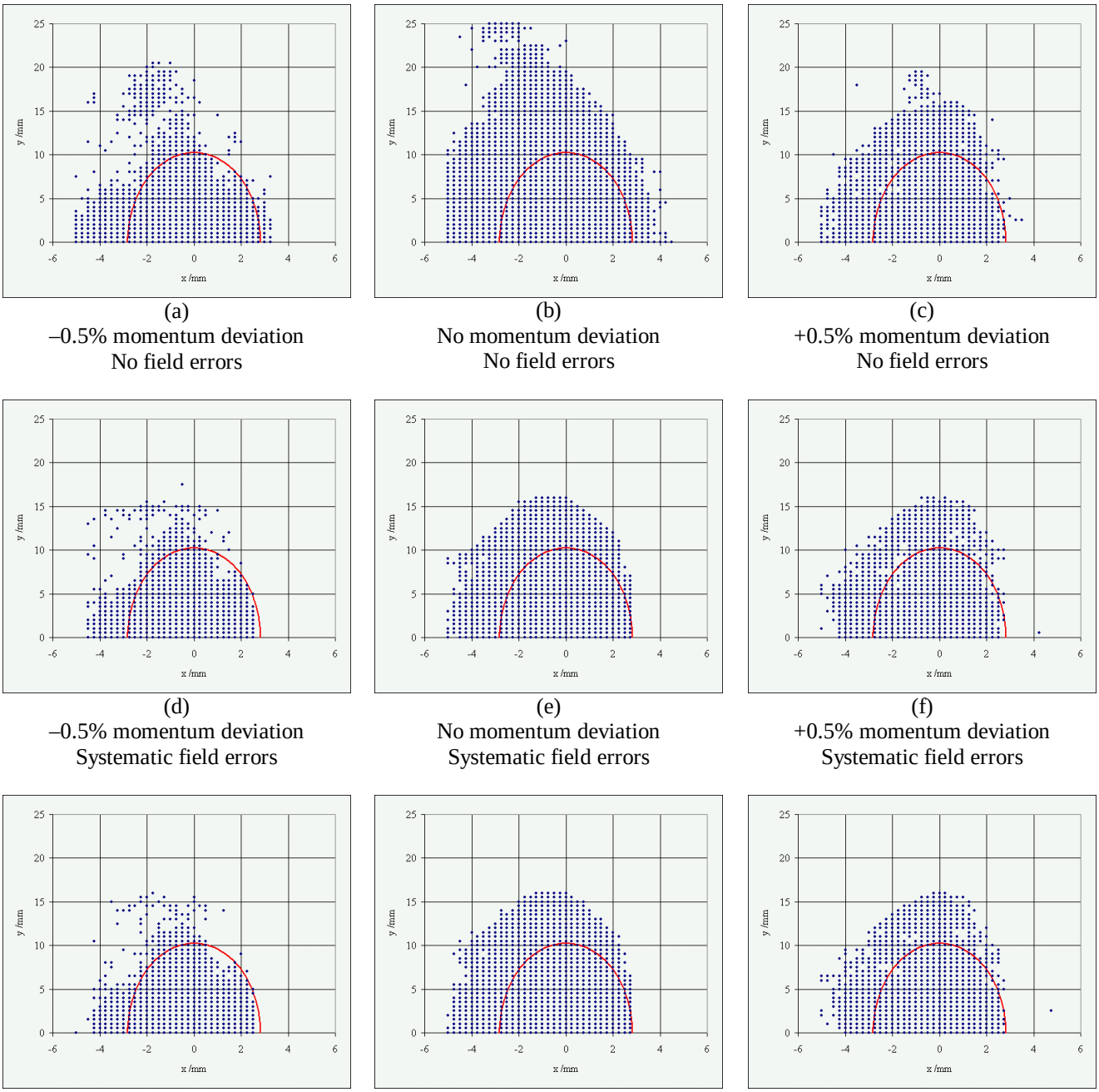

(a)
–0.5% momentum deviation
No field errors

(b)
No momentum deviation
No field errors

(c)
+0.5% momentum deviation
No field errors

(d)
–0.5% momentum deviation
Systematic field errors

(e)
No momentum deviation
Systematic field errors

(f)
+0.5% momentum deviation
Systematic field errors

(g)
-0.5% momentum deviation
Systematic and random field errors

(h)
No momentum deviation
Systematic and random field errors

(i)
+0.5% momentum deviation
Systematic and random field errors

Figure 7

Dynamic aperture of the NLC Main Damping Ring under various conditions. The points show stable orbits at the observation point (β_x=0.911 m, β_y=.911 m, η_x=0.0548 m), and the half-ellipse shows fifteen times the injected beam size (target dynamic aperture).

The results show that the dynamic aperture for on-momentum particles, and particles with up to ±0.5% momentum deviation is close to (or larger than) the target of fifteen times the injected beam size in all cases. After some reduction in the dynamic aperture from the systematic errors, the random errors appear to have relatively little effect. The principal reason for this is that the dynamic aperture observed with the systematic errors gives the region over which the particle motion is close to linear; particles whose motion is significantly nonlinear and are barely stable in the case of the "ideal" magnets are quickly lost, and adding further errors has little effect. As expected, increasing the sizes of the random errors does not have a dramatic impact. Nonetheless, we feel that the random errors we have used may be rather conservative, and the effects of more realistic errors should be explored, with the aim of specifying construction tolerances on the higher-order multipoles.

Note that we have used a linear model for the damping wiggler, which is represented as a sequence of dipoles with no higher harmonic content. Effects of nonlinearities in the wiggler have been studied previously [4], and indications are that the present wiggler design will not significantly limit the dynamic aperture. More rigorous studies of nonlinear dynamics of the wiggler are in progress [5], and when complete, a more careful evaluation of dynamics in the full lattice, including errors in the multipoles, can be performed.

5 Conclusions

Present designs for the principal magnets in the NLC Main Damping Rings suggest that the systematic higher-order multipole components will allow an acceptable dynamic aperture. Indications are that the dynamic aperture will remain sufficient in the presence of reasonable random errors arising from construction tolerances, although we have not yet set any limits on these. The magnets have been modeled using two-dimensional fields, and it is possible that edge effects could be significant, particularly for the sextupoles where the pole-tip radius is nearly half the magnetic length. Future studies will consider optimization of the three-dimensional model, and quantify the effects on the dynamics.

The work has been carried out using a linear model for the wiggler. Further detailed studies of the dynamics in the full lattice should be carried out when studies of the nonlinear wiggler model have been completed.

References

[1] A. Wolski, "Lattice Design for NLC Main Damping Rings at 120 Hz Repetition Rate", LCC-0061, April 2001.

[2] J.-Y. Jung, "Summary of LBL/SLAC Design Work on NLC Magnets", LCC-0077, October 2001.

[3] Y. Nosochkov and J. Corbett, "Dynamic Aperture Studies for SPEAR 3", SLAC-PUB-7965, October 1998.

[4] A. Wolski, "Symplectic Integrators for Nonlinear Wiggler Fields", LCC-0062, April 2001.

[5] M. Venturini, "Analysis of Single-Particle Dynamics in the NLC and TESLA Damping Ring Wigglers", in preparation.